



## Synthesis, characterization and catalytic evaluation of BiCl<sub>3</sub>-ZrO<sub>2</sub> for the synthesis of novel pyrazolyl chalcones



Saima Tarannum, Zeba N. Siddiqui \*

Department of Chemistry, Aligarh Muslim University, Aligarh 202002, India

### ARTICLE INFO

#### Article history:

Received 16 March 2014

Received in revised form 5 July 2014

Accepted 11 July 2014

Available online 21 July 2014

#### Keywords:

BiCl<sub>3</sub>-ZrO<sub>2</sub>

Heterogeneous catalyst

Pyrazolyl chalcones

Solvent-free reaction.

### ABSTRACT

BiCl<sub>3</sub>-ZrO<sub>2</sub> as an efficient heterogeneous catalyst is prepared by a simple process and characterized by FT-IR, powder XRD, SEM-EDX, XRF and BET surface area analyses. Thermal stability of the catalyst has been examined by DSC-TG analyses. The catalyst is recyclable for several runs preserving its high activity. The catalytic activity of BiCl<sub>3</sub>-ZrO<sub>2</sub> is explained by synthesizing a series of novel pyrazolyl chalcones in excellent yields.

© 2014 Elsevier B.V. All rights reserved.

## 1. Introduction

BiCl<sub>3</sub> is an acid catalyst in homogeneous medium. A wide variety of reactions in homogeneous phase employing BiCl<sub>3</sub> as efficient catalyst is reported in literature [1–4]. Though there are numerous advantages, the major drawbacks of BiCl<sub>3</sub>, as catalyst lie in its low thermal stability, risks in handling, containment, disposal and regeneration due to its toxic and corrosive nature, and difficulties in separation from reaction mixture. Therefore, heterogenization of BiCl<sub>3</sub> with suitable catalyst support is an efficient way to find new environmentally friendly catalyst with high catalytic potential [5]. It is pertinent to mention that heterogeneous catalysts are environmentally benign, easily separable, reusable, and also exhibit high catalytic activities towards different types of reactions [6–8]. Moreover, various heterogeneous catalysts used in Claisen-Schmidt condensation for the synthesis of chalcones include sulfonic acid functionalized mesoporous silicas [9], aminopropylated silica [10], sulfated Degussa titania [11], natural phosphate [12], metal-organic framework [13], NaNO<sub>3</sub>/hydroxyapatite [14], silica-H<sub>2</sub>SO<sub>4</sub> [15], Mo<sub>10</sub>V<sub>2</sub>/SiO<sub>2</sub> [16], calcined sodium nitrate/natural phosphate [17], boron trifluoride-etherate [18], BF<sub>3</sub>·SiO<sub>2</sub> [19] etc.

It is worth mentioning that substituted pyrazoles form an exclusive class of heterocyclic compounds having remarkable bioactivities such as anxiolytic, antihyperglycemic, analgesic,

anticancer, antioxidant, antimicrobial, anti-inflammatory, antidepressant and anticonvulsant etc., [20–23] and also find applications as dyestuffs, analytical reagents and applied as ligands for the transition-metal-catalyzed cross-coupling reactions [24–26]. Linking of pyrazole with a structurally diverse side chain containing heterocyclic ring is an effective way to obtain heterocyclic derivatives with high biological potential. In this context, pyrazolyl chalcones find applications as antimicrobial, anti-inflammatory, antioxidant and cytotoxic agents etc. [27,28]. Hence, an environmentally benign methodology for the preparation of such compounds is of great concern in synthetic organic chemistry.

In recent decades, zirconia has attracted much attention as a catalyst support because of its high thermal and mechanical stability, large surface area, amphoteric character and oxidizing-reducing properties [29–31]. Thus, synthesis of zirconia based solid acids has become an intellectual goal of researchers, due to its proven advantages such as non-hazardous nature, improved surface properties, enhanced catalytic activity and recyclability. Taking into consideration the prospective use of zirconia as catalyst support and BiCl<sub>3</sub> as a reaction promoter herein, we wish to report an efficient synthesis of zirconia supported BiCl<sub>3</sub> at ambient temperature. The structure, morphology and stability of the catalyst was established with the help of FT-IR spectrum, powder x-ray diffraction (XRD), scanning electron microscopy (SEM), energy dispersive x-ray analysis (EDX), x-ray fluorescence (XRF), Brunauer–Emmett–Teller (BET) surface area analysis, differential scanning calorimetry (DSC) and thermo-gravimetric analysis (TGA). The catalytic activity of the catalyst was explained by synthesizing pyrazolyl chalcones via Claisen–Schmidt condensation involving energy sustainable

\* Corresponding author. Tel.: +91 9412653054.

E-mail addresses: [siddiqui\\_zeba@yahoo.co.in](mailto:siddiqui_zeba@yahoo.co.in), [zns.siddiqui@gmail.com](mailto:zns.siddiqui@gmail.com) (Z.N. Siddiqui).

methodology. All pyrazolyl chalcones were identified on the basis of spectral data (FT-IR, NMR and mass spectrometry).

## 2. Experimental

### 2.1. Chemicals and apparatus

Melting points of all synthesized compounds were taken in a Riechert Thermover instrument and are uncorrected. The IR spectra (KBr) were recorded on Perkin Elmer RXI spectrometer. <sup>1</sup>H NMR and <sup>13</sup>C NMR spectra were recorded on a Bruker DRX-300 and Bruker Avance II 400 spectrometer using tetramethylsilane (TMS) as an internal standard and DMSO-d<sub>6</sub>/CDCl<sub>3</sub> as solvent. ESI-MS was recorded on a Quattro II (ESI) spectrometer. Elemental analyses (C, H and N) were conducted using the Elemental vario EL III elemental analyzer and their results were found to be in agreement with the calculated values. 5-chloro-3-methyl-1-phenylpyrazole-4-carbaldehyde and 5-aryloxy-3-methyl-1-phenylpyrazole-4-carbaldehyde were synthesized by reported procedures [32,33]. Other chemicals were of commercial grade and used without further purification. The homogeneity of the compounds was checked by thin layer chromatography (TLC) on glass plates coated with silica gel G254 (E. Merck) using chloroform-methanol (3:1) mixture as mobile phase and visualized using iodine vapors. X-ray diffractograms (XRD) of the catalyst were recorded in the 2θ range of 10–80° with scan rate of 4°/min on a Rigaku Minifax X-ray diffractometer with Ni-filtered Cu Kα radiation at a wavelength of 1.54060 Å. SEM-EDX characterization of the catalyst was performed on a JEOL JSM-6510 scanning electron microscope equipped with energy dispersive x-ray spectrometer operating at 20 kV. DSC data was obtained with DSC-60 and TGA with DTG-60H (Simultaneous DTA-TG Apparatus), Shimadzu instrument. X-ray fluorescence analysis was carried out with a PHILLIPS PW 2404. BET surface area of the sample was measured from the nitrogen adsorption/desorption isotherms obtained by using a Quantachrome Autosorb 1 C BET analyzer at 77 K temperature. Prior to gas adsorption, the sample was degassed for 3 h at 423 K.

### 2.2. Preparation of catalyst (BiCl<sub>3</sub>-ZrO<sub>2</sub>)

Zirconia (20 g) was activated by refluxing with HCl (6 M, 100 mL) under stirring for 24 h. It was filtered, washed with double distilled water and dried under vacuum at 70 °C for 24 h.

A mixture of activated zirconia (4.00 g) and bismuth (III) chloride (1.00 g) in toluene was stirred at room temperature overnight, filtered off and washed with ethanol. The solid, as obtained was dried at 120 °C under vacuum for 6 h as white powder.

### 2.3. General procedure for the preparation of products 5a–t

A mixture of 5- aryloxy-3-methyl-1-phenylpyrazole-4-carbaldehydes **3a–d** (10 mmol), active methyl ketones **4a–e** (10 mmol), and 0.8 g of BiCl<sub>3</sub>-ZrO<sub>2</sub> (20% w/w) was heated at 80 °C. Upon completion of the reaction (as confirmed by TLC) the reaction mixture was cooled to room temperature and ethyl acetate (5 mL) was added. The reaction mixture was filtered to remove the catalyst and filtrate concentrated to furnish products **5a–t** which was further purified by recrystallization with suitable solvents.

### 2.4. Spectroscopic Data

**5a** (2E)-3-(3-methyl-5-phenoxy-1-phenylpyrazol-4-yl)-1-(1,3-dimethyl-2,4,6-pyrimidinetrione-5-yl)-2-propen-1-one

Yellow crystals; M.p: 185–190 °C. IR (KBr) ( $\nu_{\text{max}}$ , cm<sup>-1</sup>): 1650 (C=O), 1716 (C=O). <sup>1</sup>H NMR (DMSO-d<sub>6</sub>, 400 MHz):  $\delta$  2.52 (s, 3H,

CH<sub>3</sub>), 3.36 (s, 6H, 2 × NCH<sub>3</sub>), 6.96–8.27 (m, 10H, Ar-H), 8.27 (d, 1H,  $J$ =16.0 Hz, H<sub>b</sub>), 8.32 (d, 1H,  $J$ =15.6 Hz, H<sub>a</sub>). <sup>13</sup>C NMR (100 MHz):  $\delta$  14.36, 27.34, 115.29, 117.49, 121.96, 123.98, 127.62, 129.17, 130.07, 134.32, 136.66, 148.15, 149.29, 155.48, 176.23, 182.70. ESI-MS (m/z) 459.14 (M<sup>+</sup> + 1). Anal. Calcd (C<sub>25</sub>H<sub>22</sub>N<sub>4</sub>O<sub>5</sub>): C, 65.49; H, 4.83; N, 12.22. Anal. Found (C<sub>25</sub>H<sub>22</sub>N<sub>4</sub>O<sub>5</sub>): C, 65.54; H, 4.88; N, 12.16.

**5b** (2E)-3-(3-methyl-5-phenoxy-1-phenylpyrazol-4-yl)-1-(2,4,6-pyrimidinetrione-5-yl)-2-propen-1-one

Light yellow crystals; M.p: 260–265 °C. IR (KBr) ( $\nu_{\text{max}}$ , cm<sup>-1</sup>): 1677 (C=O), 1729 (C=O), 3184 (NH). <sup>1</sup>H NMR (DMSO-d<sub>6</sub>, 400 MHz):  $\delta$  2.51 (s, 3H, CH<sub>3</sub>), 6.92–7.80 (m, 10H, Ar-H), 8.19 (d, 1H,  $J$ =15.8 Hz, H<sub>b</sub>), 8.24 (d, 1H,  $J$ =15.6 Hz, H<sub>a</sub>), 11.28 (s, 2H, 2 × NH). <sup>13</sup>C NMR (100 MHz):  $\delta$  13.67, 116.24, 121.36, 122.66, 122.88, 124.34, 127.90, 128.12, 131.24, 135.86, 139.18, 150.82, 154.64, 176.17, 187.49. ESI-MS (m/z) 431.1 (M<sup>+</sup> + 1). Anal. Calcd (C<sub>23</sub>H<sub>18</sub>N<sub>4</sub>O<sub>5</sub>): C, 64.18; H, 4.21; N, 13.01. Anal. Found (C<sub>23</sub>H<sub>18</sub>N<sub>4</sub>O<sub>5</sub>): C, 64.13; H, 4.26; N, 13.07.

**5c** (2E)-3-(3-methyl-5-phenoxy-1-phenylpyrazol-4-yl)-1-(2-mercaptop-4,6-pyrimidinedione-5-yl)-2-propen-1-one

Light yellow crystals; M.p: 280–285 °C. IR (KBr) ( $\nu_{\text{max}}$ , cm<sup>-1</sup>): 1059 (C=S), 1674 (C=O), 1726 (C=O), 3039 (NH). <sup>1</sup>H NMR (DMSO-d<sub>6</sub>, 400 MHz):  $\delta$  2.50 (s, 3H, CH<sub>3</sub>), 6.95–7.66 (m, 10H, Ar-H), 8.17 (d, 1H,  $J$ =16.0 Hz, H<sub>a</sub>), 8.17 (d, 1H,  $J$ =16.0 Hz, H<sub>b</sub>), 12.22 (s, 1H, NH), 12.73 (s, 1H, NH). <sup>13</sup>C NMR (100 MHz):  $\delta$  13.96, 106.15, 116.09, 117.45, 121.97, 123.44, 128.64, 129.46, 130.57, 134.32, 137.40, 148.24, 150.24, 156.18, 177.04, 181.35. ESI-MS (m/z) 447.1 (M<sup>+</sup> + 1). Anal. Calcd (C<sub>23</sub>H<sub>18</sub>N<sub>4</sub>O<sub>4</sub>S): C, 61.87; H, 4.06; N, 12.54. Anal. Found (C<sub>23</sub>H<sub>18</sub>N<sub>4</sub>O<sub>4</sub>S): C, 61.84; H, 4.12; N, 12.48.

**5d** (2E)-1-(4-hydroxy-6-methyl-2-oxo-2H-pyran-3-yl)-3-(3-methyl-5-phenoxy-1-phenylpyrazol-4-yl)-2-propen-1-one

Light orange crystals; M.p: 180–185 °C. IR (KBr) ( $\nu_{\text{max}}$ , cm<sup>-1</sup>): 1646 (C=O), 1734 (C=O), 3103 (OH). <sup>1</sup>H NMR (DMSO-d<sub>6</sub>, 400 MHz):  $\delta$  2.24 (s, 3H, CH<sub>3</sub>), 2.52 (s, 3H, CH<sub>3</sub>), 5.94 (s, 1H, CH), 7.25–7.58 (m, 10H, Ar-H), 7.88 (d, 1H,  $J$ =16.0 Hz, H<sub>b</sub>), 8.06 (d, 1H,  $J$ =16.0 Hz, H<sub>a</sub>), 18.72 (s, 1H, OH). <sup>13</sup>C NMR (100 MHz):  $\delta$  14.29, 24.45, 106.35, 115.29, 117.49, 123.98, 127.62, 130.07, 134.32, 136.66, 148.15, 154.72, 155.48, 160.24, 162.82, 176.28, 181.34. ESI-MS (m/z) 429.60 (M<sup>+</sup> + 1). Anal. Calcd (C<sub>25</sub>H<sub>20</sub>N<sub>2</sub>O<sub>5</sub>): C, 70.08; H, 4.70; N, 6.53. Anal. Found (C<sub>25</sub>H<sub>20</sub>N<sub>2</sub>O<sub>5</sub>): C, 70.01; H, 4.65; N, 6.55.

**5e** (2E)-1-(4-hydroxy-1-benzopyran-2-one-3-yl)-3-(3-methyl-5-phenoxy-1-phenylpyrazol-4-yl)-2-propen-1-one

Yellow crystals; M.p: 220–225 °C. IR (KBr) ( $\nu_{\text{max}}$ , cm<sup>-1</sup>): 1648 (C=O), 1731 (C=O), 3074 (OH). <sup>1</sup>H NMR (DMSO-d<sub>6</sub>, 400 MHz):  $\delta$  2.53 (s, 3H, CH<sub>3</sub>), 6.97–8.00 (m, 14H, Ar-H), 8.02 (d, 1H,  $J$ =16.0 Hz, H<sub>a</sub>), 8.10 (d, 1H,  $J$ =15.9 Hz, H<sub>b</sub>), 18.95 (s, 1H, OH). <sup>13</sup>C NMR (100 MHz):  $\delta$  13.36, 104.18, 106.26, 113.96, 115.29, 117.49, 123.98, 125.68, 128.82, 130.64, 134.76, 136.12, 148.28, 153.12, 155.52, 160.74, 162.20, 176.09, 182.12. ESI-MS (m/z) 465.47 (M<sup>+</sup> + 1). Anal. Calcd (C<sub>28</sub>H<sub>20</sub>N<sub>2</sub>O<sub>5</sub>): C, 72.40; H, 4.34; N, 6.03. Anal. Found (C<sub>28</sub>H<sub>20</sub>N<sub>2</sub>O<sub>5</sub>): C, 72.32; H, 4.30; N, 6.07.

**5f** (2E)-3-(3-methyl-5-(4-nitrophenoxy)-1-phenylpyrazol-4-yl)-1-(1,3-dimethyl-2,4,6-pyrimidinetrione-5-yl)-2-propen-1-one

Yellow crystals; M.p: 225–230 °C. IR (KBr) ( $\nu_{\text{max}}$ , cm<sup>-1</sup>): 1662 (C=O), 1714 (C=O). <sup>1</sup>H NMR (DMSO-d<sub>6</sub>, 400 MHz):  $\delta$  2.51 (s, 3H, CH<sub>3</sub>), 3.32 (s, 6H, 2 × NCH<sub>3</sub>), 7.23–7.86 (m, 9H, Ar-H), 8.23 (d, 1H,  $J$ =16.4 Hz, H<sub>b</sub>), 8.53 (d, 1H,  $J$ =16.2 Hz, H<sub>a</sub>). <sup>13</sup>C NMR (100 MHz):  $\delta$  14.22, 27.08, 117.14, 117.64, 121.34, 122.38, 126.42, 129.47, 131.79, 134.56, 137.04, 148.19, 149.63, 156.24, 175.64, 180.44. ESI-MS (m/z) 504.1 (M<sup>+</sup> + 1). Anal. Calcd (C<sub>25</sub>H<sub>21</sub>N<sub>5</sub>O<sub>7</sub>): C, 59.64; H, 4.20; N, 13.91. Anal. Found (C<sub>25</sub>H<sub>21</sub>N<sub>5</sub>O<sub>7</sub>): C, 59.60; H, 4.27; N, 13.78.

**5g** (2E)-3-(3-methyl-5-(4-nitrophenoxy)-1-phenylpyrazol-4-yl)-1-(2,4,6-pyrimidinetrione-5-yl)-2-propen-1-one

Yellow crystals; M.p: 220–225 °C. IR (KBr) ( $\nu_{\text{max}}$ , cm<sup>-1</sup>): 1645 (C=O), 1698 (C=O), 3194 (NH). <sup>1</sup>H NMR (DMSO-d<sub>6</sub>, 400 MHz):  $\delta$  2.48 (s, 3H, CH<sub>3</sub>), 6.88–7.92 (m, 9H, Ar-H), 8.12 (d, 1H,  $J$ =16.0 Hz, H<sub>b</sub>), 8.20 (d, 1H,  $J$ =16.2 Hz, H<sub>a</sub>), 12.02 (s, 2H, 2 × NH). <sup>13</sup>C NMR (100 MHz):  $\delta$  13.82, 116.14, 121.22, 122.60, 123.24, 123.41, 127.80,

128.46, 129.49, 130.84, 136.06, 139.38, 149.32, 154.14, 175.74, 186.14. ESI-MS (*m/z*) 476.1 ( $M^+ + 1$ ). Anal. Calcd ( $C_{23}H_{17}N_5O_7$ ): C, 58.10; H, 3.60; N, 14.73. Anal. Found ( $C_{23}H_{17}N_5O_7$ ): C, 58.17; H, 3.69; N, 14.65.

**5h** (2E)-3-(3-methyl-5-(4-nitrophenoxy)-1-phenylpyrazol-4-yl)-1-(2-mercaptopro-4,6-pyrimidinedione-5-yl)-2-propen-1-one

Yellow crystals; M.p: 235–240 °C. IR (KBr) ( $\nu_{max}$ , cm<sup>-1</sup>): 1150 (C=S), 1650 (C=O), 1670 (C=O), 3184 (NH). <sup>1</sup>H NMR (DMSO-*d*<sub>6</sub>, 400 MHz):  $\delta$  2.52 (s, 3H, CH<sub>3</sub>), 6.85–7.86 (m, 9H, Ar-H), 8.32 (d, 1H, *J*=15.8 Hz, Ha), 9.00 (d, 1H, *J*=15.8 Hz, Hb), 11.46 (s, 1H, NH), 11.66 (s, 1H, NH). <sup>13</sup>C NMR (100 MHz):  $\delta$  13.88, 106.22, 116.24, 118.44, 121.12, 123.52, 127.69, 129.48, 130.37, 133.74, 137.92, 149.35, 150.41, 156.13, 177.26, 180.32. ESI-MS (*m/z*) 492.1 ( $M^+ + 1$ ). Anal. Calcd ( $C_{23}H_{17}N_5O_6S$ ): C, 56.20; H, 3.48; N, 14.25. Anal. Found ( $C_{23}H_{17}N_5O_6S$ ): C, 56.26; H, 3.41; N, 14.20.

**5i** (2E)-1-(4-hydroxy-6-methyl-2-oxo-2H-pyran-3-yl)-3-(3-methyl-5-(4-nitrophenoxy)-1-phenylpyrazol-4-yl)-2-propen-1-one

Yellow crystals; M.p: 195–200 °C. IR (KBr) ( $\nu_{max}$ , cm<sup>-1</sup>): 1644 (C=O), 1698 (C=O), 3194 (OH). <sup>1</sup>H NMR (DMSO-*d*<sub>6</sub>, 400 MHz):  $\delta$  2.28 (s, 3H, CH<sub>3</sub>), 2.50 (s, 3H, CH<sub>3</sub>), 5.86 (s, 1H, CH), 6.98–7.64 (m, 9H, Ar-H), 7.78 (d, 1H, *J*=16.2 Hz, Hb), 8.00 (d, 1H, *J*=15.8 Hz, Ha), 18.21 (s, 1H, OH). <sup>13</sup>C NMR (100 MHz):  $\delta$  14.34, 23.88, 105.46, 116.84, 118.16, 123.20, 128.16, 132.72, 134.64, 136.82, 147.56, 149.47, 154.53, 155.48, 160.28, 162.74, 176.24, 181.92. ESI-MS (*m/z*) 474.43 ( $M^+ + 1$ ). Anal. Calcd ( $C_{25}H_{19}N_3O_7$ ): C, 63.42; H, 4.04; N, 8.87. Anal. Found ( $C_{25}H_{19}N_3O_7$ ): C, 63.34; H, 4.09; N, 8.78.

**5j** (2E)-1-(4-hydroxy-1-benzopyran-2-one-3-yl)-3-(3-methyl-5-(4-nitrophenoxy)-1-phenylpyrazol-4-yl)-2-propen-1-one

Yellow crystals; M.p: 200–205 °C. IR (KBr) ( $\nu_{max}$ , cm<sup>-1</sup>): 1639 (C=O), 1666 (C=O), 3115 (OH). <sup>1</sup>H NMR (DMSO-*d*<sub>6</sub>, 400 MHz):  $\delta$  2.51 (s, 3H, CH<sub>3</sub>), 6.97–8.05 (m, 13H, Ar-H), 8.06 (d, 1H, *J*=16.0 Hz, Ha), 8.24 (d, 1H, *J*=16.0 Hz, Hb), 18.88 (s, 1H, OH). <sup>13</sup>C NMR (100 MHz):  $\delta$  14.04, 104.23, 105.45, 113.82, 115.29, 118.63, 124.15, 126.44, 128.06, 128.14, 130.22, 132.80, 134.32, 136.72, 148.32, 153.30, 155.08, 159.82, 162.14, 175.26, 181.28. ESI-MS (*m/z*) 510.54 ( $M^+ + 1$ ). Anal. Calcd ( $C_{28}H_{19}N_3O_7$ ): C, 66.01; H, 3.75; N, 8.24. Anal. Found ( $C_{28}H_{19}N_3O_7$ ): C, 66.10; H, 3.68; N, 8.21.

**5k** (2E)-3-(3-methyl-5-(4-methoxyphenoxy)-1-phenylpyrazol-4-yl)-1-(1,3-dimethyl-2,4,6-pyrimidinetrione-5-yl)-2-propen-1-one

Yellow crystals; M.p: 185–190 °C. IR (KBr) ( $\nu_{max}$ , cm<sup>-1</sup>): 1650 (C=O), 1714 (C=O). <sup>1</sup>H NMR (DMSO-*d*<sub>6</sub>, 400 MHz):  $\delta$  2.52 (s, 3H, CH<sub>3</sub>), 3.15 (s, 6H, 2  $\times$  NCH<sub>3</sub>), 3.73 (s, 3H, OCH<sub>3</sub>), 6.83–7.35 (m, 9H, Ar-H), 7.47 (d, 1H, *J*=15.8 Hz, Hb), 7.65 (d, 1H, *J*=16.5 Hz, Ha). <sup>13</sup>C NMR (100 MHz):  $\delta$  13.88, 27.48, 54.04, 116.85, 118.65, 120.66, 122.14, 127.35, 129.63, 131.82, 132.96, 136.92, 148.43, 148.74, 156.06, 175.24, 181.34. ESI-MS (*m/z*) 489.1 ( $M^+ + 1$ ). Anal. Calcd ( $C_{26}H_{24}N_4O_6$ ): C, 63.92; H, 4.95; N, 11.46. Anal. Found ( $C_{26}H_{24}N_4O_6$ ): C, 63.96; H, 4.92; N, 11.42.

**5l** (2E)-3-(3-methyl-5-(4-methoxyphenoxy)-1-phenylpyrazol-4-yl)-1-(2,4,6-pyrimidinetrione-5-yl)-2-propen-1-one

Light yellow crystals; M.p: 220–225 °C. IR (KBr) ( $\nu_{max}$ , cm<sup>-1</sup>): 1662 (C=O), 1715 (C=O), 3146 (NH). <sup>1</sup>H NMR (DMSO-*d*<sub>6</sub>, 400 MHz):  $\delta$  2.50 (s, 3H, CH<sub>3</sub>), 3.56 (s, 3H, OCH<sub>3</sub>), 6.98–8.02 (m, 9H, Ar-H), 8.02 (d, 1H, *J*=15.8 Hz, Ha), 8.08 (d, 1H, *J*=15.6 Hz, Hb), 11.74 (s, 2H, 2  $\times$  NH). <sup>13</sup>C NMR (100 MHz):  $\delta$  13.62, 53.68, 116.14, 121.25, 122.76, 124.38, 127.12, 128.37, 129.52, 131.04, 136.46, 138.12, 148.32, 151.54, 154.40, 173.14, 184.28. ESI-MS (*m/z*) 461.1 ( $M^+ + 1$ ). Anal. Calcd ( $C_{24}H_{20}N_4O_6$ ): C, 62.60; H, 4.37; N, 12.16. Anal. Found ( $C_{24}H_{20}N_4O_6$ ): C, 62.64; H, 4.27; N, 12.11.

**5m** (2E)-3-(3-methyl-5-(4-methoxyphenoxy)-1-phenylpyrazol-4-yl)-1-(2-mercaptopro-4,6-pyrimidinedione-5-yl)-2-propen-1-one

Light yellow crystals; M.p: 230–235 °C. IR (KBr) ( $\nu_{max}$ , cm<sup>-1</sup>): 1007 (C=S), 1678 (C=O), 1714 (C=O), 3126 (NH). <sup>1</sup>H NMR

(DMSO-*d*<sub>6</sub>, 400 MHz):  $\delta$  2.52 (s, 3H, CH<sub>3</sub>), 3.45 (s, 3H, OCH<sub>3</sub>), 6.85–7.96 (m, 9H, Ar-H), 8.08 (d, 1H, *J*=15.8 Hz, Hb), 8.12 (d, 1H, *J*=15.8 Hz, Ha), 11.36 (s, 1H, NH), 11.60 (s, 1H, NH). <sup>13</sup>C NMR (100 MHz):  $\delta$  13.88, 54.10, 106.22, 116.24, 118.44, 121.12, 123.52, 127.69, 129.48, 130.37, 133.74, 137.92, 149.35, 150.41, 156.13, 177.26, 180.32. ESI-MS (*m/z*) 477.1 ( $M^+ + 1$ ). Anal. Calcd ( $C_{24}H_{20}N_4O_5S$ ): C, 60.49; H, 4.23; N, 11.75. Anal. Found ( $C_{24}H_{20}N_4O_5S$ ): C, 60.44; H, 4.28; N, 11.73.

**5n** (2E)-1-(4-hydroxy-6-methyl-2-oxo-2H-pyran-3-yl)-3-(3-methyl-5-(4-methoxyphenoxy)-1-phenylpyrazol-4-yl)-2-propen-1-one

Light orange crystals; M.p: 210–215 °C. IR (KBr) ( $\nu_{max}$ , cm<sup>-1</sup>): 1658 (C=O), 1709 (C=O), 3167 (OH). <sup>1</sup>H NMR (DMSO-*d*<sub>6</sub>, 400 MHz):  $\delta$  2.25 (s, 3H, CH<sub>3</sub>), 2.51 (s, 3H, CH<sub>3</sub>), 3.42 (s, 3H, OCH<sub>3</sub>), 5.95 (s, 1H, CH), 7.24–7.76 (m, 9H, Ar-H), 7.96 (d, 1H, *J*=15.6 Hz, Hb), 8.02 (d, 1H, *J*=15.8 Hz, Ha), 18.14 (s, 1H, OH). <sup>13</sup>C NMR (100 MHz):  $\delta$  14.34, 24.45, 53.18, 105.12, 115.64, 117.54, 123.12, 127.44, 130.72, 134.64, 135.86, 149.24, 154.72, 155.48, 156.92, 160.54, 163.74, 175.18, 180.90. ESI-MS (*m/z*) 459.64 ( $M^+ + 1$ ). Anal. Calcd ( $C_{26}H_{22}N_2O_6$ ): C, 68.11; H, 4.83; N, 6.11. Anal. Found ( $C_{26}H_{22}N_2O_6$ ): C, 68.15; H, 4.88; N, 6.02.

**5o** (2E)-1-(4-hydroxy-1-benzopyran-2-one-3-yl)-3-(3-methyl-5-(4-methoxyphenoxy)-1-phenylpyrazol-4-yl)-2-propen-1-one

Yellow crystals; M.p: 210–215 °C. IR (KBr) ( $\nu_{max}$ , cm<sup>-1</sup>): 1634 (C=O), 1718 (C=O), 3134 (OH). <sup>1</sup>H NMR (DMSO-*d*<sub>6</sub>, 400 MHz):  $\delta$  2.51 (s, 3H, CH<sub>3</sub>), 3.43 (s, 3H, OCH<sub>3</sub>), 6.97–8.02 (m, 13H, Ar-H), 8.02 (d, 1H, *J*=16.0 Hz, Ha), 8.06 (d, 1H, *J*=16.3 Hz, Hb), 18.92 (s, 1H, OH). <sup>13</sup>C NMR (100 MHz):  $\delta$  13.46, 53.04, 105.12, 106.16, 113.92, 115.17, 118.34, 124.64, 125.12, 128.18, 130.12, 130.32, 132.45, 134.46, 136.64, 148.72, 154.25, 156.46, 159.34, 160.62, 176.48, 180.60. ESI-MS (*m/z*) 495.82 ( $M^+ + 1$ ). Anal. Calcd ( $C_{29}H_{22}N_2O_6$ ): C, 70.43; H, 4.48; N, 5.66. Anal. Found ( $C_{29}H_{22}N_2O_6$ ): C, 70.37; H, 4.41; N, 5.69.

**5p** (2E)-3-(3-methyl-5-(4-chlorophenoxy)-1-phenylpyrazol-4-yl)-1-(1,3-dimethyl-2,4,6-pyrimidinetrione-5-yl)-2-propen-1-one

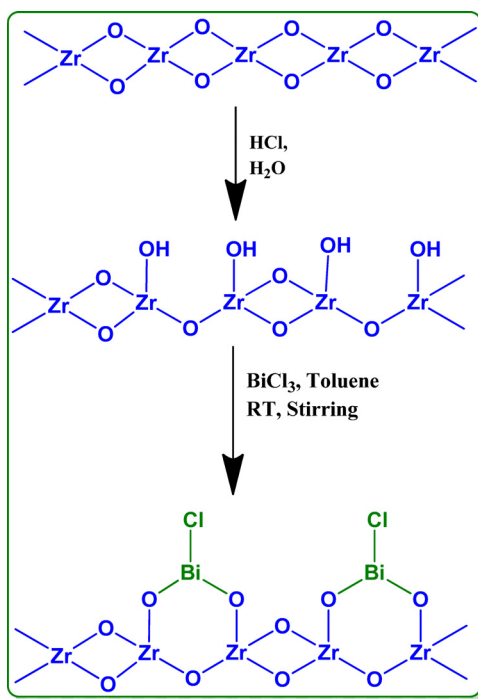
Yellow crystals; M.p: 200–205 °C. IR (KBr) ( $\nu_{max}$ , cm<sup>-1</sup>): 1662 (C=O), 1714 (C=O). <sup>1</sup>H NMR (DMSO-*d*<sub>6</sub>, 400 MHz):  $\delta$  2.50 (s, 3H, CH<sub>3</sub>), 3.20 (s, 6H, 2  $\times$  NCH<sub>3</sub>), 6.82–7.41 (m, 9H, Ar-H), 7.45 (d, 1H, *J*=15.8 Hz, Hb), 7.63 (d, 1H, *J*=16.0 Hz, Ha). <sup>13</sup>C NMR (100 MHz):  $\delta$  14.12, 26.96, 116.24, 117.44, 121.66, 123.12, 126.62, 129.61, 130.07, 134.73, 135.68, 149.14, 149.20, 155.26, 176.68, 180.94. ESI-MS (*m/z*) 493.1 ( $M^+ + 1$ ). Anal. Calcd ( $C_{25}H_{21}ClN_4O_5$ ): C, 60.91; H, 4.29; N, 11.36. Anal. Found ( $C_{25}H_{21}ClN_4O_5$ ): C, 60.97; H, 4.21; N, 11.28.

**5q** (2E)-3-(3-methyl-5-(4-chlorophenoxy)-1-phenylpyrazol-4-yl)-1-(2,4,6-pyrimidinetrione-5-yl)-2-propen-1-one

Light yellow crystals; M.p: 225–230 °C. IR (KBr) ( $\nu_{max}$ , cm<sup>-1</sup>): 1645 (C=O), 1700 (C=O), 3103 (NH). <sup>1</sup>H NMR (DMSO-*d*<sub>6</sub>, 400 MHz):  $\delta$  2.49 (s, 3H, CH<sub>3</sub>), 6.92–7.86 (m, 9H, Ar-H), 8.00 (d, 1H, *J*=15.6 Hz, Hb), 8.05 (d, 1H, *J*=16.0 Hz, Ha), 11.64 (s, 2H, 2  $\times$  NH). <sup>13</sup>C NMR (100 MHz):  $\delta$  14.04, 117.25, 121.02, 122.14, 123.31, 127.82, 128.46, 129.24, 130.84, 136.02, 139.35, 149.40, 150.32, 154.56, 174.92, 185.12. ESI-MS (*m/z*) 465.1 ( $M^+ + 1$ ). Anal. Calcd ( $C_{23}H_{17}ClN_4O_5$ ): C, 59.42; H, 3.68; N, 12.05. Anal. Found ( $C_{23}H_{17}ClN_4O_5$ ): C, 59.47; H, 3.62; N, 12.12.

**5r** (2E)-3-(3-methyl-5-(4-chlorophenoxy)-1-phenylpyrazol-4-yl)-1-(2-mercaptopro-4,6-pyrimidinedione-5-yl)-2-propen-1-one

Light yellow crystals; M.p: 240–245 °C. IR (KBr) ( $\nu_{max}$ , cm<sup>-1</sup>): 1087 (C=S), 1662 (C=O), 1700 (C=O), 3108 (NH). <sup>1</sup>H NMR (DMSO-*d*<sub>6</sub>, 400 MHz):  $\delta$  2.56 (s, 3H, CH<sub>3</sub>), 7.45–8.02 (m, 9H, Ar-H), 8.06 (d, 1H, *J*=15.8 Hz, Hb), 8.10 (d, 1H, *J*=15.7 Hz, Ha), 11.46 (s, 1H, NH), 11.72 (s, 1H, NH). <sup>13</sup>C NMR (100 MHz):  $\delta$  14.04, 105.89, 116.64, 117.74, 121.68, 122.72, 127.39, 128.18, 131.06, 133.26, 138.14, 151.26, 157.32, 176.20, 182.06. ESI-MS (*m/z*) 481.1 ( $M^+ + 1$ ). Anal. Calcd ( $C_{23}H_{17}ClN_4O_4S$ ): C, 57.44; H, 3.56; N, 11.65. Anal. Found ( $C_{23}H_{17}ClN_4O_4S$ ): C, 57.42; H, 3.48; N, 11.59.

**Scheme 1.** Synthesis of catalyst  $\text{BiCl}_3\text{-ZrO}_2$ .

**5s** (2E)-1-(4-hydroxy-6-methyl-2-oxo-2H-pyran-3-yl)-3-(3-methyl-5-(4-chlorophenoxy)-1-phenylpyrazol-4-yl)-2-propen-1-one

Light orange crystals; M.p: 180–185 °C. IR (KBr) ( $\nu_{\text{max}}$ ,  $\text{cm}^{-1}$ ): 1632 (C=O), 1688 (C=O), 3182 (OH).  $^1\text{H}$  NMR (DMSO- $d_6$ , 400 MHz): 2.26 (s, 3H,  $\text{CH}_3$ ), 2.50 (s, 3H,  $\text{CH}_3$ ), 5.94 (s, 1H, CH), 7.14–7.64 (m, 9H, Ar-H), 7.88 (d, 1H,  $J$ =15.6 Hz, Hb), 7.90 (d, 1H,  $J$ =15.8 Hz, Ha), 18.36 (s, 1H, OH).  $^{13}\text{C}$  NMR (100 MHz):  $\delta$  13.86, 22.10, 104.64, 116.72, 118.14, 124.04, 127.28, 130.28, 135.12, 136.84, 148.26, 154.16, 155.92, 160.74, 162.46, 175.56, 180.46. ESI-MS ( $m/z$ ) 463.32 ( $\text{M}^+ + 1$ ). Anal. Calcd (C<sub>25</sub>H<sub>19</sub>ClN<sub>2</sub>O<sub>5</sub>): C, 64.86; H, 4.13; N, 6.05. Anal. Found (C<sub>25</sub>H<sub>19</sub>ClN<sub>2</sub>O<sub>5</sub>): C, 64.81; H, 4.18; N, 6.13.

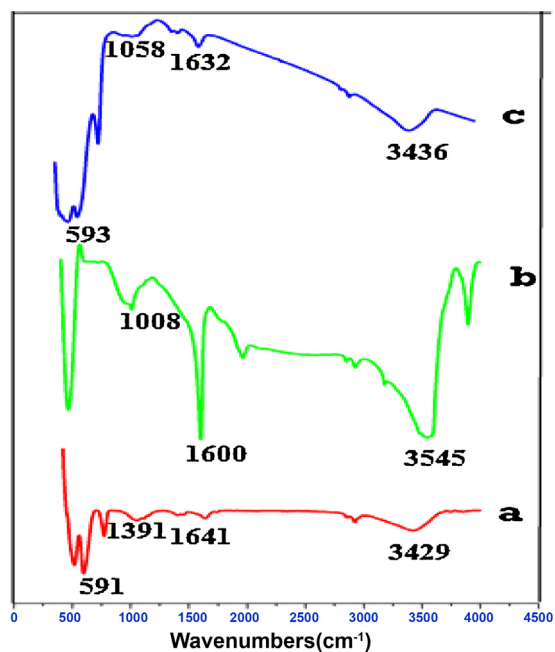
**5t** (2E)-1-(4-hydroxy-1-benzopyran-2-one-3-yl)-3-(3-methyl-5-(4-chlorophenoxy)-1-phenylpyrazol-4-yl)-2-propen-1-one

Yellow crystals; M.p: 190–195 °C. IR (KBr) ( $\nu_{\text{max}}$ ,  $\text{cm}^{-1}$ ): 1620 (C=O), 1712 (C=O), 3125 (OH).  $^1\text{H}$  NMR (DMSO- $d_6$ , 400 MHz):  $\delta$  2.51 (s, 3H,  $\text{CH}_3$ ), 6.97–7.77 (m, 13H, Ar-H), 8.00 (d, 1H,  $J$ =16.0 Hz, Ha), 8.08 (d, 1H,  $J$ =15.9 Hz, Hb), 18.95 (s, 1H, OH).  $^{13}\text{C}$  NMR (100 MHz):  $\delta$  14.36, 104.56, 105.68, 114.26, 115.72, 118.26, 125.05, 126.92, 128.62, 129.24, 131.76, 132.14, 134.18, 136.45, 148.74, 154.26, 155.59, 159.17, 162.34, 175.19, 182.16. ESI-MS ( $m/z$ ) 499.74 ( $\text{M}^+ + 1$ ). Anal. Calcd (C<sub>28</sub>H<sub>19</sub>ClN<sub>2</sub>O<sub>5</sub>): C, 67.40; H, 3.83; N, 5.61. Anal. Found (C<sub>28</sub>H<sub>19</sub>ClN<sub>2</sub>O<sub>5</sub>): C, 67.32; H, 3.76; N, 5.65.

### 3. Results and discussion

#### 3.1. Catalyst synthesis and characterization

$\text{BiCl}_3\text{-ZrO}_2$  was prepared by stirring  $\text{BiCl}_3$  in a suspension of activated zirconia in toluene at room temperature overnight (Scheme 1). The chloride content of the catalyst was determined by Mohr titration. In this method, the sample solution was titrated against a solution of silver nitrate of known concentration (0.1 M) using  $\text{K}_2\text{CrO}_4$  as an indicator. The results showed that 2 chloride ions per  $\text{BiCl}_3$  were released during the synthesis of the catalyst. This suggested the presence of  $\text{BiCl}$  instead of  $\text{BiCl}_3$  in the synthesized catalytic system.

**Fig. 1.** FT-IR Spectra of (a)  $\text{ZrO}_2$ , (b)  $\text{BiCl}_3$  and (c)  $\text{BiCl}_3\text{-ZrO}_2$ .

#### 3.1.1. FT-IR spectrum of $\text{BiCl}_3\text{-ZrO}_2$

The FT-IR spectrum of  $\text{ZrO}_2$  (Fig. 1a) showed a broad asymmetric stretching band in the region of 3429  $\text{cm}^{-1}$  due to OH-group. Weak bands at 1641 and 1391  $\text{cm}^{-1}$  were due to  $-(\text{H}-\text{O}-\text{H})$ -bending and  $-(\text{O}-\text{H}-\text{O})$ -bending vibrations. A weak bending band at 591  $\text{cm}^{-1}$  was attributed to  $\text{Zr}-\text{O}-\text{H}$  bond. In spectrum of  $\text{BiCl}_3$  (Fig. 1b), absorption peaks at 1600 and 1008  $\text{cm}^{-1}$  indicated the asymmetric and symmetric stretching vibrations of  $\text{Bi}-\text{Cl}$  bond. A sharper absorption band of OH-group at 3545  $\text{cm}^{-1}$  in  $\text{BiCl}_3$  was appeared due to its strong hygroscopic property. The FT-IR spectrum of catalyst (Fig. 1c) showed peaks corresponding to both  $\text{ZrO}_2$  and  $\text{BiCl}_3$ . A broad band in the region of 3436  $\text{cm}^{-1}$  was assigned to  $(-\text{OH})$  stretching vibration, whereas bands at 1632 and 1058  $\text{cm}^{-1}$  were due to asymmetric and symmetric stretching vibrations of  $\text{Bi}-\text{Cl}$  respectively. A broad absorption band at 593  $\text{cm}^{-1}$  was attributed to bending vibration of  $\text{Zr}-\text{O}-\text{Bi}$  bond.

#### 3.1.2. Powder x-ray diffraction (XRD) analysis of $\text{BiCl}_3\text{-ZrO}_2$

The XRD patterns of the support and supported catalyst showed crystallinity and sharper peaks. XRD pattern of pure zirconia (Fig. 2a) can be described as the sum of the monoclinic and tetragonal phases of zirconia. It is an established fact that  $\text{ZrO}_2$ -tetragonal phase is more active in catalysis [34]. For  $\text{BiCl}_3\text{-ZrO}_2$ , new peaks appeared in the region of 10–30° showed that tetragonal phase becoming dominant for zirconia supported with  $\text{BiCl}_3$  (Fig. 2b).

#### 3.1.3. SEM-EDX analysis of the catalyst

For the morphology of catalyst, SEM image of 20%  $\text{BiCl}_3\text{-ZrO}_2$  (Fig. 3a and b) showed non-uniform distribution of the particles with agglomerates.

EDX analysis of the catalyst revealed peaks for Bi, Cl, Zr and O indicating formation of the expected catalytic system (Fig. 4).

#### 3.1.4. XRF analysis of the catalyst

Elemental analysis of  $\text{BiCl}_3\text{-ZrO}_2$  was performed by means of x-ray fluorescence (XRF) analysis (Table 1). The chemical/elemental analysis of  $\text{BiCl}_3\text{-ZrO}_2$  indicated that  $\text{ZrO}_2$  content was 76.82 wt % whereas Bi and Cl contents were 8.75 wt %, 0.62 wt % respectively.

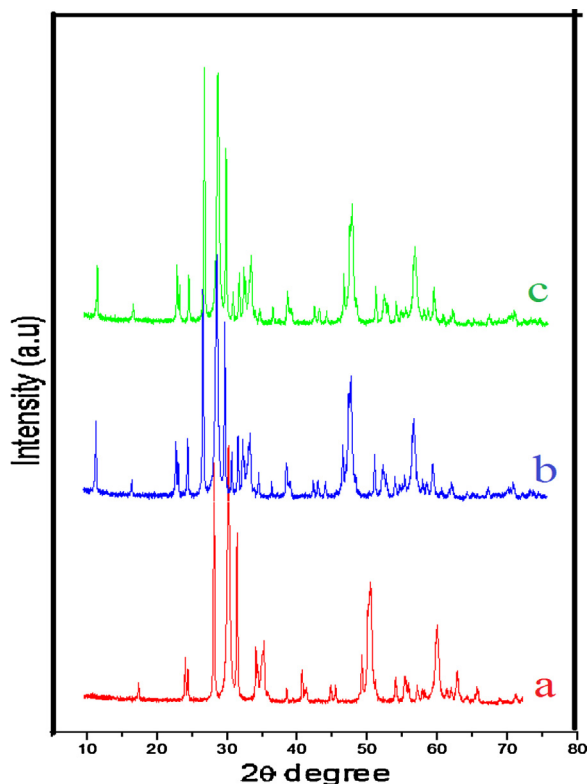


**Fig. 2.** (a) The powder XRD pattern of zirconia (b) XRD pattern of fresh catalyst ( $\text{BiCl}_3\text{-ZrO}_2$ ) (c) XRD pattern of the catalyst after six catalytic cycles.

**Table 1**  
Summary of composition of  $\text{BiCl}_3\text{-ZrO}_2$  determined by XRF analysis.

Catalyst	Composition of catalyst by XRF		
	$\text{ZrO}_2$	Bi	Cl
$\text{BiCl}_3\text{-ZrO}_2$	76.82	8.75	0.62

Further, Cl/Bi weight ratio and Bi/ZrO<sub>2</sub> weight ratio were found to be 0.07 and 0.11 respectively.

### 3.1.5. BET surface area analysis

Brunauer–Emmett–Teller (BET) surface areas of ZrO<sub>2</sub>, activated ZrO<sub>2</sub> and BiCl<sub>3</sub>-ZrO<sub>2</sub> are given in Fig. 5. The surface area of the activated ZrO<sub>2</sub> and BiCl<sub>3</sub>-ZrO<sub>2</sub> catalyst are  $24 \text{ m}^2 \text{ g}^{-1}$  and  $21.9 \text{ m}^2 \text{ g}^{-1}$ , as expected, higher than that of the bulk ZrO<sub>2</sub> material ( $1.8 \text{ m}^2 \text{ g}^{-1}$ ). The decrease in surface area of the BiCl<sub>3</sub> loaded ZrO<sub>2</sub> in comparison

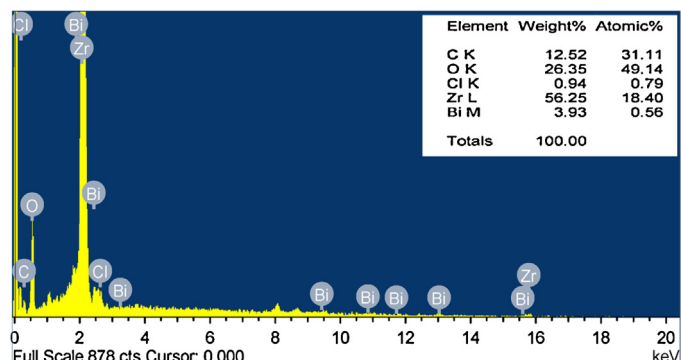


**Fig. 4.** EDX analysis of the catalyst ( $\text{BiCl}_3\text{-ZrO}_2$ ).

to activated ZrO<sub>2</sub> indicates filling of some of the pores by the BiCl<sub>3</sub> component preventing N<sub>2</sub> adsorption in the filled pores.

The pore volumes for ZrO<sub>2</sub>, activated ZrO<sub>2</sub> and BiCl<sub>3</sub>-ZrO<sub>2</sub> obtained were 0.0026, 0.0339 and  $0.033 \text{ ccg}^{-1}$  respectively.

### 3.1.6. DSC-TGA of catalyst ( $\text{BiCl}_3\text{-ZrO}_2$ )

DSC analysis of BiCl<sub>3</sub>-ZrO<sub>2</sub> showed an irreversible endothermic peak at  $100^\circ\text{C}$  indicating the loss of water molecules from zirconia framework (Fig. 6a). The catalyst did not show any other transition up to  $500^\circ\text{C}$  indicating the stability of the catalyst up to this temperature.

A significant decrease in the weight percentage of 5.57 (up to  $250^\circ\text{C}$ ) as evident from the TG curve (Fig. 6b) was attributed to the loss of adsorbed moisture on the surface of the catalyst. In addition, weight loss of 6.60% at  $\sim 700^\circ\text{C}$  showed the transformation of BiCl<sub>3</sub> to its oxide at higher temperatures.

## 3.2. Catalytic evaluation

The catalytic activity of BiCl<sub>3</sub>-ZrO<sub>2</sub> was evaluated using model reaction of 3-methyl-5-phenoxy-1-phenylpyrazole-4-carbaldehyde (1 mmol) and 5-acetyl-1,3-dimethyl-2,4,6-pyrimidinetrione (1 mmol). The effect of various catalysts, solvents, percentage of BiCl<sub>3</sub> loading, amount of BiCl<sub>3</sub>-ZrO<sub>2</sub> and temperature were studied to optimize the reaction condition.

### 3.2.1. Effect of different catalysts

Initially, a blank reaction was carried out using 1 equiv. each of active methyl compound (**4a**) and aldehyde (**3a**). These reactants were stirred at  $80^\circ\text{C}$  under solvent-free conditions for 8 h and only 22% of the yield of the product (**5a**) was obtained (Table 2, entry 1).

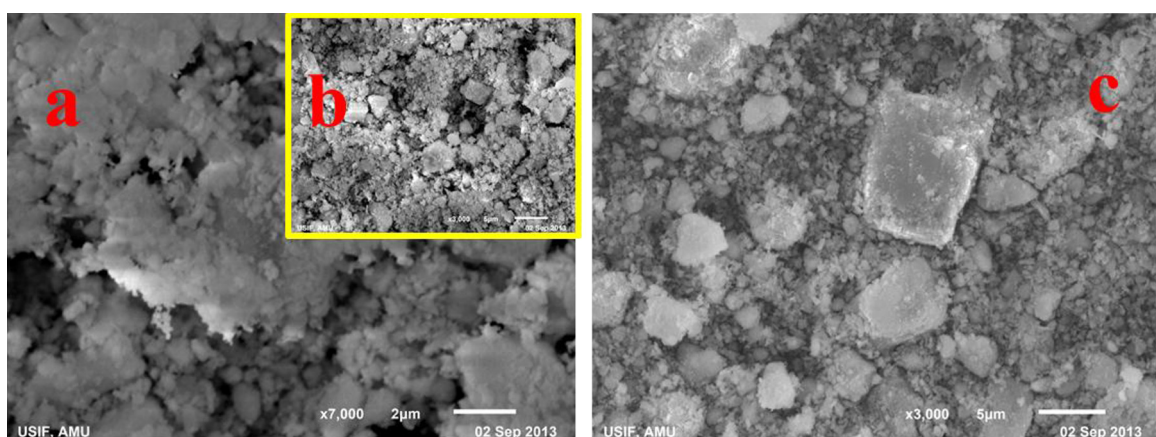


**Fig. 3.** SEM images (a and b) of fresh catalyst ( $\text{BiCl}_3\text{-ZrO}_2$ ) and (c) of recycled catalyst.

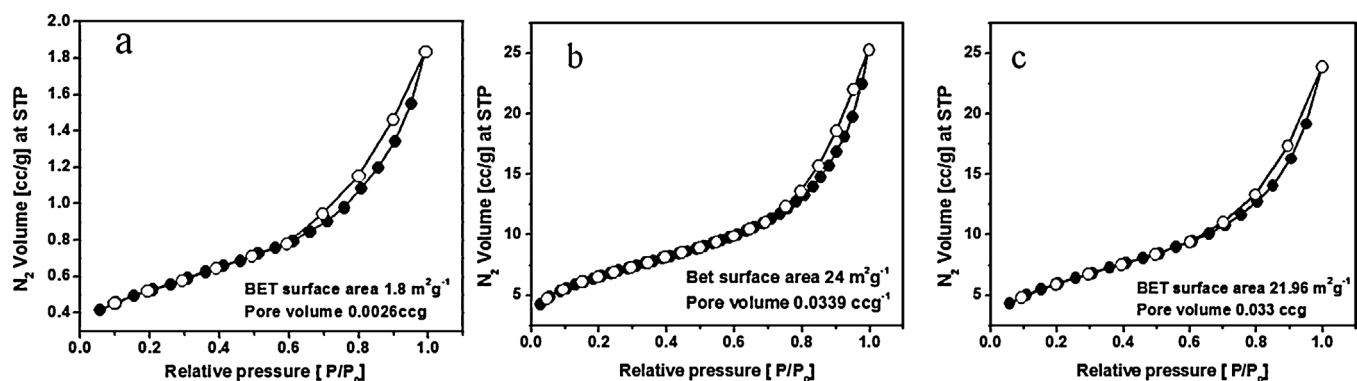


Fig. 5. Nitrogen adsorption isotherm and pore volume analysis of (a) ZrO<sub>2</sub> (b) activated ZrO<sub>2</sub> and (c) BiCl<sub>3</sub>-ZrO<sub>2</sub>.

**Table 2**

The effect of various catalysts on the model reaction under thermal solvent-free condition.

Entry <sup>a</sup>	Catalyst	Time <sup>b</sup>	Yield <sup>c</sup> (%)
1	–	8 h	22
2	ZrO <sub>2</sub>	4 h	Trace
3	FeCl <sub>3</sub>	2 h	48
4	NiCl <sub>2</sub>	1 h	54
5	ZnCl <sub>2</sub>	1 h	46
6	BiNO <sub>3</sub>	3 h	26
7	AlCl <sub>3</sub>	2 h	Trace
8	CuCl <sub>2</sub>	6 h	25
9	Sulfated zirconia	50 min	62
10	BiCl <sub>3</sub>	2.5 h	68
11	BiCl <sub>3</sub> -SiO <sub>2</sub>	30 min	90
12	BiCl <sub>3</sub> -TiO <sub>2</sub>	3 h	42
13	BiCl <sub>3</sub> -ZrO <sub>2</sub>	15 min	92

<sup>a</sup> Reaction of 3-methyl-5-phenoxy-1-phenylpyrazole-4-carbaldehyde (1 mmol) with 5-acetyl-1,3-dimethyl-2,4,6-pyrimidinetrione (1 mmol) in the presence of 80 mg of catalyst.

<sup>b</sup> Reaction progress monitored by TLC.

<sup>c</sup> Isolated yield.

The same reaction was then carried out using ZrO<sub>2</sub> as the promoter and again trace amount of the product was obtained (Table 2, entry 2). Using FeCl<sub>3</sub>, NiCl<sub>2</sub> and ZnCl<sub>2</sub>, reaction completed in 1–2 h but with unsatisfactory product yield (Table 2, entries 3–5). BiNO<sub>3</sub>, AlCl<sub>3</sub> and CuCl<sub>2</sub> also could not give satisfactory results (Table 2, entries 6–8). Sulfated zirconia and BiCl<sub>3</sub> afforded products only in moderate yield (Table 2, entries 9, 10). When the reaction was carried out using BiCl<sub>3</sub> loaded on silica (BiCl<sub>3</sub>-SiO<sub>2</sub>) good yield (90%) of the product was obtained in 30 min (Table 2, entry 11) but with BiCl<sub>3</sub> loaded on titania ((BiCl<sub>3</sub>-TiO<sub>2</sub>) poor yield (42%) of the

**Table 3**

Solvent effect on the synthesis of **5a** in the presence of BiCl<sub>3</sub>-ZrO<sub>2</sub>.

Entry <sup>a</sup>	Solvent	Time <sup>b</sup>	Yield <sup>c</sup>
1	H <sub>2</sub> O	16 h	22
2	CH <sub>3</sub> CH <sub>2</sub> COOCH <sub>3</sub>	20 h	45
3	CH <sub>3</sub> CN	16 h	49
4	CH <sub>2</sub> Cl <sub>2</sub>	18 h	48
5	THF	18 h	45
6	CH <sub>3</sub> OH	7 h	78
7	CH <sub>3</sub> CH <sub>2</sub> OH	9 h	74
8	(CH <sub>3</sub> ) <sub>2</sub> CHOH	9 h	72
9	No solvent	15 min	92

<sup>a</sup> Reaction of 3-methyl-5-phenoxy-1-phenylpyrazole-4-carbaldehyde (1 mmol) with 5-acetyl-1,3-dimethyl-2,4,6-pyrimidinetrione (1 mmol) in the presence of BiCl<sub>3</sub>-ZrO<sub>2</sub> (80 mg).

<sup>b</sup> Reaction progress monitored by TLC.

<sup>c</sup> Isolated yield.

product was obtained after 3 h (Table 2, entry 12). However, maximum yield of the product was obtained using BiCl<sub>3</sub>-ZrO<sub>2</sub> as the catalyst (Table 2, entry 13).

### 3.2.2. Effect of solvents

In our initial selection, we used BiCl<sub>3</sub>-ZrO<sub>2</sub> in water for the model reaction but product was obtained with trace yield (Table 3, entry 1). Using ethyl acetate, acetonitrile, dichloromethane, tetrahydrofuran, only moderate yields were obtained (Table 3, entries 2–5). In polar solvents CH<sub>3</sub>OH, CH<sub>3</sub>CH<sub>2</sub>OH and (CH<sub>3</sub>)<sub>2</sub>CHOH, product formation increased to some extent but with unsatisfactory yield (Table 3, entries 6–8). In this study, it was observed that solvent-free condition (Table 3, entry 9) was more efficient and superior condition with respect to reaction time and yield.

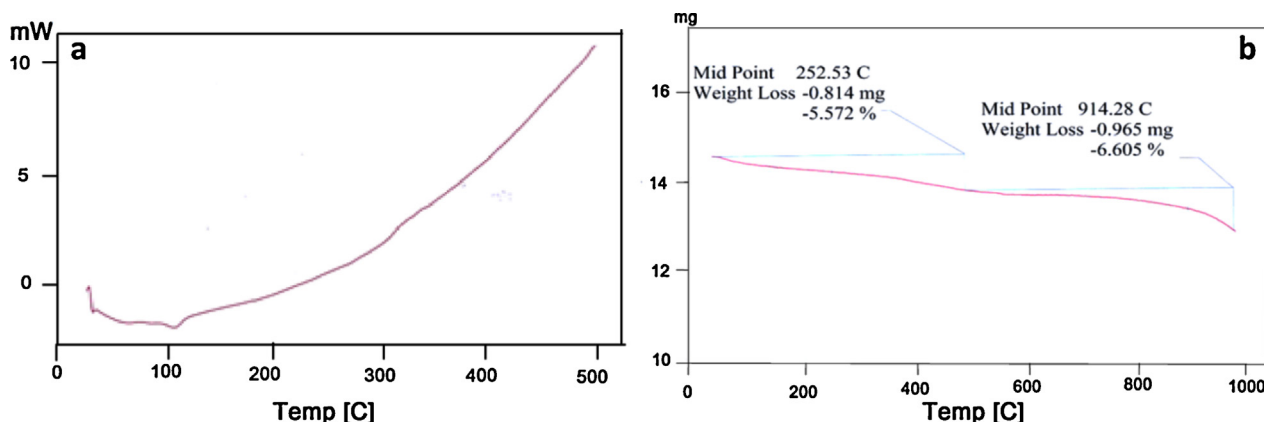


Fig. 6. (a) DSC of catalyst (b) TG curve of catalyst (BiCl<sub>3</sub>-ZrO<sub>2</sub>).

**Table 4**Effect of  $\text{BiCl}_3$  loading on support  $\text{ZrO}_2$  for the synthesis of **5a**.

Entry <sup>a</sup>	$\text{BiCl}_3\text{-ZrO}_2$ (%w/w)	Time <sup>b</sup>	Yield <sup>c</sup> (%)
1	7	1.2 h	64
2	10	1 h	76
3	15	45 min	82
4	20	15 min	92
5	25	15 min	90

<sup>a</sup> Reaction of 3-methyl-5-phenoxy-1-phenylpyrazole-4-carbaldehyde (1 mmol) with 5-acetyl-1,3-dimethyl-2,4,6-pyrimidinetrione (1 mmol) in the presence of  $\text{BiCl}_3\text{-ZrO}_2$  (80 mg).

<sup>b</sup> Reaction progress monitored by TLC.

<sup>c</sup> Isolated yield.

**Table 5**Effect of amount of catalyst on the synthesis of **5a** in thermal solvent-free condition.

Entry	$\text{BiCl}_3\text{-ZrO}_2$ (mg)	Time <sup>a</sup>	Yield <sup>b</sup>
1	20	1.5 h	54
2	40	1 h	68
3	60	40 min	94
4	80	15 min	92
5	100	15 min	92

<sup>a</sup> Reaction progress monitored by TLC.

<sup>b</sup> Isolated yield.

### 3.2.3. Effect of loading of the catalyst

The catalyst loading was varied as 7, 10, 15, 20 and 25% w/w of  $\text{BiCl}_3$  supported on  $\text{ZrO}_2$  (**Table 4**). With increase in catalyst loading, the yield was found to increase up to 20% further increase has no effect on the yield. The optimum catalyst loading was thus taken as 20%.

### 3.2.4. Effect of the amount of catalyst

Similarly, amount of catalyst was varied from 20 to 100 mg, the yield was found to increase with increase in amount up to 80 mg, and further increase in amount did not improve the product yield and reaction time (**Table 5**). The optimum amount of catalyst for the reaction was selected as 80 mg.

### 3.2.5. Effect of temperature

The reaction temperature is an important factor which affects the reaction rate under solvent-free condition. The increase of temperature can enhance stimulation of molecules leading to improvement of product yield and reaction time. As shown in **Table 6**, the effect of this variable was positive relevant to temperature from 25 °C to 80 °C. Further, increase in the temperature reduced the time period but with the formation of a charred product. Therefore, the optimum temperature was found to be 80 °C and employed in the experiment.

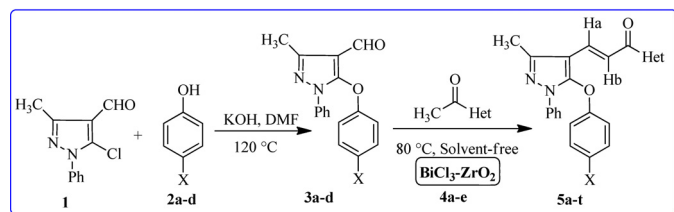
**Table 6**Effect of temperature on the synthesis of **5a** in solvent-free condition.

Entry <sup>a</sup>	Temperature	Time <sup>b</sup>	Yield <sup>c</sup>
1	RT	–	–
2	40 °C	5 h	58
3	60 °C	2.5 h	72
4	80 °C	15 min	92
5	100 °C	10 min	64

<sup>a</sup> Reaction of 3-methyl-5-phenoxy-1-phenylpyrazole-4-carbaldehyde (1 mmol) with 5-acetyl-1,3-dimethyl-2,4,6-pyrimidinetrione (1 mmol) in the presence of  $\text{BiCl}_3\text{-ZrO}_2$  (80 mg).

<sup>b</sup> Reaction progress monitored by TLC.

<sup>c</sup> Isolated yield.



X=	3a	3b	3c	3d
	H	NO <sub>2</sub>	OCH <sub>3</sub>	Cl
4a	4b	4c	4d	4e

**Scheme 2.** Synthesis of pyrazolyl chalcones (**5a-t**) using  $\text{BiCl}_3\text{-ZrO}_2$  under thermal solvent-free conditions.

### 3.3. Synthesis of pyrazolyl chalcones via Claisen–Schmidt condensation in the presence of $\text{BiCl}_3\text{-ZrO}_2$

To explore general validity of our methodology,  $\text{BiCl}_3\text{-ZrO}_2$  was employed for the synthesis of series of pyrazolyl chalcones (**5a-t**) using substituted aldehydes (**3a-d**) and heterocyclic active methyl ketones (**4a-e**) under the optimized reaction conditions (**Scheme 2**). The reaction proceeded efficiently and afforded products in excellent yields (86–92%) in a short span of time period (15–25 min) (**Table 7**).

The structure of all novel compounds (**5a-t**) was confirmed on the basis of spectral analysis (FT-IR, <sup>1</sup>H NMR, <sup>13</sup>C NMR and mass spectra). The infrared (IR) spectrum of **5a** showed sharp and strong absorption bands of carbonyl group of barbituric and propenone moiety at 1716 cm<sup>-1</sup> and 1650 cm<sup>-1</sup> respectively. Another sharp and strongly absorbed band at 1615 cm<sup>-1</sup> was due to carbon–carbon double bond of  $\alpha$ ,  $\beta$ -unsaturated system. The <sup>1</sup>H NMR spectrum showed trans olefinic protons Ha and Hb at  $\delta$  8.32 ( $J$  = 15.6 Hz) and  $\delta$  8.27 ( $J$  = 16.0 Hz), as two ortho-coupled doublets. The value of spin–spin coupling constant  $J_{ab}$  in the range 15–16 Hz indicated the E-configuration of chalcone. The aromatic protons of the pyrazole moiety were present in the form of multiplet at  $\delta$  6.96–8.27. Two NCH<sub>3</sub> group protons of barbituric acid moiety were discernible as sharp singlet at  $\delta$  3.36 whereas protons of CH<sub>3</sub> group of pyrazole unit appeared as another sharp singlet at  $\delta$  2.52. The <sup>13</sup>C NMR spectrum showed signals at  $\delta$  176.23 and 27.34 for carbonyl and methyl group of 1,3-dimethyl barbituric acid respectively. Another signal at  $\delta$  182.70 was for carbonyl group of  $\alpha$ ,  $\beta$ -unsaturated system. Other carbon signals appeared at their appropriate positions and are discussed in experimental section. Further confirmation for **5a** was obtained by mass spectrum, which showed molecular ion peak as M<sup>+</sup> + 1 peak at m/z 459.14.

A general plausible mechanism for synthesis of pyrazolyl chalcones in the presence of  $\text{BiCl}_3\text{-ZrO}_2$  has been shown in **Scheme 3**.

### 3.4. Reusability of catalyst

To establish the heterogeneous character of the catalyst, recycling experiment was employed using model reaction. After completion of reaction, the catalyst was recovered by filtration, washed with ethanol and dried under vacuum. The recovered catalyst was reused for six cycles with a minor loss in catalytic activity (**Fig. 7**).

**Table 7**

The reaction of 5-aryloxy-3-methyl-1-phenyl-pyrazole-4-carbaldehydes and cyclic active methyl compounds in presence of  $\text{BiCl}_3\text{-ZrO}_2$  under thermal solvent-free conditions.

Entry	Aldehyde (3a-d)	Ketone (4a-e)	Product (5a-t)	Time <sup>a</sup> (min)	Yield <sup>b</sup> (%)
1	3a	4a		15	92
2	3a	4b		20	92
3	3a	4c		20	90
4	3a	4d		17	90
5	3a	4e		20	92

Table 7 (Continued)

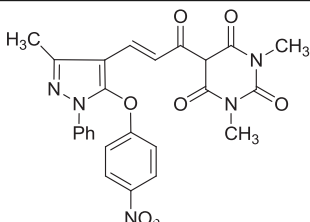
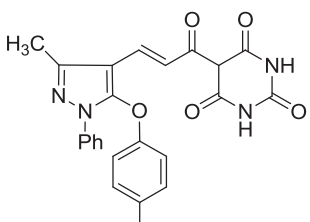
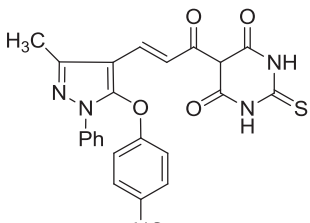
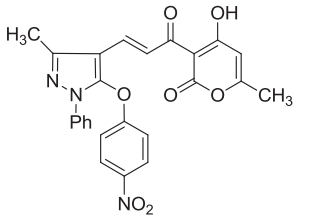
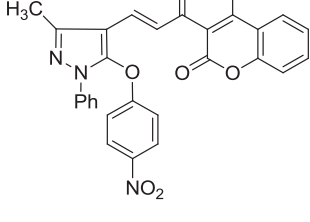
Entry	Aldehyde	Ketone	Product	Time <sup>a</sup>	Yield <sup>b</sup>
6	<b>3b</b>	<b>4a</b>		15	92
7	<b>3b</b>	<b>4b</b>		18	90
8	<b>3b</b>	<b>4c</b>		20	88
9	<b>3b</b>	<b>4d</b>		15	90
10	<b>3b</b>	<b>4e</b>		15	88

Table 7 (Continued)

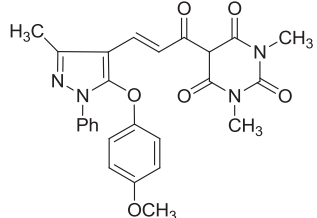
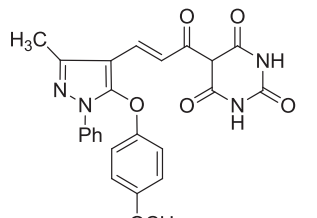
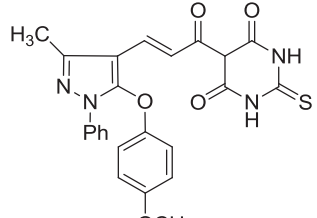
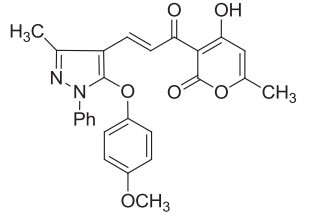
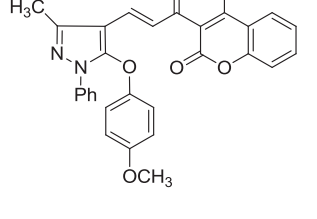
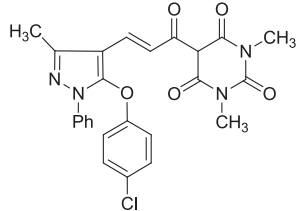
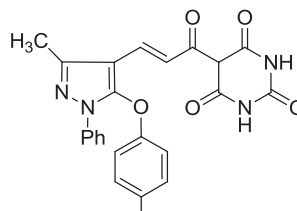
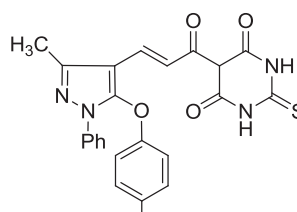
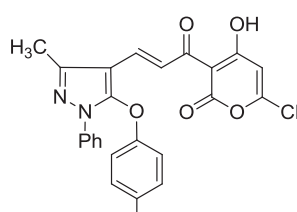
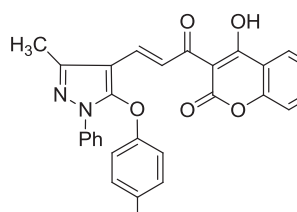
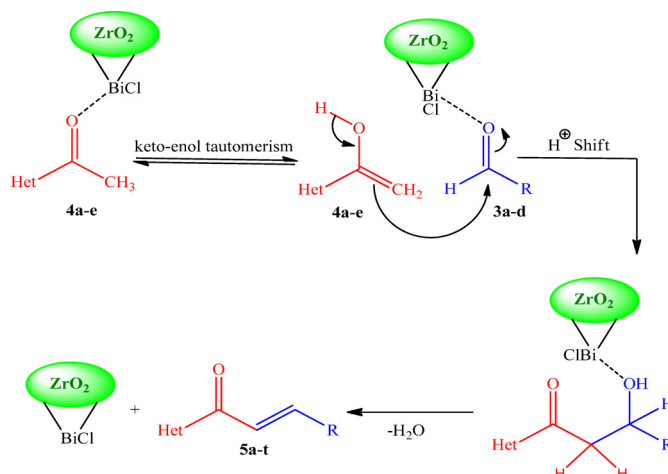
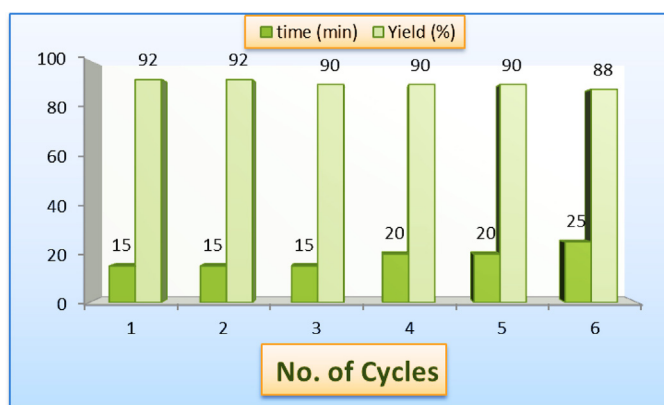
Entry	Aldehyde	Ketone	Product	Time <sup>a</sup>	Yield <sup>b</sup>
11	<b>3c</b>	<b>4a</b>		20	88
			<b>5k</b>		
12	<b>3c</b>	<b>4b</b>		25	86
			<b>5l</b>		
13	<b>3c</b>	<b>4c</b>		25	86
			<b>5m</b>		
14	<b>3c</b>	<b>4d</b>		17	90
			<b>5n</b>		
15	<b>3c</b>	<b>4e</b>		20	92
			<b>5o</b>		

Table 7 (Continued)

Entry	Aldehyde	Ketone	Product	Time <sup>a</sup>	Yield <sup>b</sup>
16	<b>3d</b>	<b>4a</b>		15	90
			<b>5p</b>		
17	<b>3d</b>	<b>4b</b>		25	86
			<b>5q</b>		
18	<b>3d</b>	<b>4c</b>		25	88
			<b>5r</b>		
19	<b>3d</b>	<b>4d</b>		20	88
			<b>5s</b>		
20	<b>3d</b>	<b>4e</b>		15	90
			<b>5t</b>		

<sup>a</sup> Reaction progress monitored by TLC.<sup>b</sup> Isolated yield.

**Scheme 3.** Proposed mechanism for the formation of  $5\text{a-t}$ .**Fig. 7.** Recyclability of the catalytic system.

The slight loss observed in the catalytic activity after 6th run could be due to temporary poisoning by organic impurities or due to minor changes in the structure and morphology of the catalyst under the operating conditions (Figs. 2c, 3c).

#### 4. Conclusion

In summary, we have synthesized and characterized heterogeneous version of  $\text{BiCl}_3$  ( $\text{BiCl}_3\text{-ZrO}_2$ ). The catalytic activity of the catalyst was explored by synthesizing a library of novel pyrazolyl chalcones in excellent yield. The wide scope, practicability, enhanced rate of reaction, operational simplicity and reusability of catalyst provide attractive approach for applications in other organic transformations in the future.

#### Acknowledgements

The authors are thankful to Centre of Nanotechnology, Department of Applied Physics and University Sophisticated Instrument Facility (USIF), AMU, Aligarh for providing powder x-ray diffractometer and SEM-EDX facilities. The authors would also like to thank SAIF, Punjab University, Chandigarh, for providing spectral data. SAIF, IIT Bombay is gratefully acknowledged for providing XRF analysis data. UGC, New Delhi, is gratefully acknowledged for awarding research fellowship to ST.

#### References

- [1] H. Li, H. Zeng, H. Shao, *Tetrahedron Lett.* 50 (2009) 6858–6860.
- [2] V.V. Kouznetsov, C.M.M. Gomez, F.A.R. Ruiz, E. del Olmo, *Tetrahedron Lett.* 53 (2012) 3115–3118.
- [3] H. Sun, R. Huia, S. Chen, Y. Yin, *Adv. Synth. Catal.* 348 (2006) 1919–1925.
- [4] D. Kumar, Suresh, J.S. Sandhu, *Green Chem. Lett. Rev.* 3 (2010) 283–286.
- [5] K. Aghapoor, L. Ebadi-Nia, F. Mohsenzadeh, M.M. Morad, Y. Balavar, H.R. Darabi, *J. Organometal. Chem.* 708–709 (2012) 25–30.
- [6] J.A. Gladysz, *Chem. Rev.* 102 (2002) 3215–3216.
- [7] A.P.S. Chouhan, A.K. Sarma, *Renew. Sust. Energ. Rev.* 15 (2011) 4378–4399.
- [8] T. Okuhara, *Chem. Rev.* 102 (2002) 3641–3666.
- [9] S. Shylesh, P.P. Samuel, C. Srivakshmi, R. Parischa, A.P. Singh, *J. Mol. Catal. A: Chem.* 274 (2007) 153–158.
- [10] G. Romanelli, G. Pasquale, A. Sathicq, H. Thomas, J. Autino, P. Vazquez, *J. Mol. Catal. A: Chem.* 340 (2011) 24–32.
- [11] B. Krishnakumar, M. Swaminathan, *J. Mol. Catal. A: Chem.* 350 (2011) 16–25.
- [12] S. Sebt, A. Saber, A. Rhihil, R. Nazih, R. Tahir, *Appl. Catal. A: Gen.* 206 (2001) 217–220.
- [13] A. Dhakshinamoorthy, M. Alvaro, H. Garcia, *Adv. Synth. Catal.* 352 (2010) 711–717.
- [14] S. Sebt, A. Solhy, R. Tahir, A. Smahi, *Appl. Catal. A: Gen.* 235 (2002) 273–281.
- [15] A. Sultan, A.R. Raza, M. Abbas, K.M. Khan, M.N. Tahir, N. Saari, *Molecules* 18 (2013) 10081–10094.
- [16] E. Rafiee, F. Rahimi, *J. Chil. Chem. Soc.* 58 (2013) 1926–1929.
- [17] S. Sebt, A. Solhy, R. Tahir, S. Boulaajaj, J.A. Mayoral, J.M. Fraile, A. Kossir, H. Oumimoun, *Tetrahedron Lett.* 42 (2001) 7953–7955.
- [18] T. Narendar, K.P. Reddy, *Tetrahedron Lett.* 48 (2007) 3177–3180.
- [19] B. Sadeghi, B.F. Mirjalili, M.M. Hashemi, *J. Iran. Chem. Soc.* 5 (2008) 694–698.
- [20] B.E. Maryanoff, D.F. Mc Comsey, W. Ho, R.P. Shank, B. Dubinsky, *Bioorg. Med. Chem. Lett.* 6 (1996) 333–338.
- [21] F.K. Keter, J. Darkwa, *Biomaterials* 25 (2012) 9–21.
- [22] D. Dewangan, T. Kumar, A. Alexander, K. Nagori, D.K. Tripathi, *CPR* 1 (2011) 369–377.
- [23] A. Chauhan, P.K. Sharma, N. Kaushik, *Int. J. Chem. Tech. Res.* 3 (2011) 11–17.
- [24] H.F. Rizk, M.A. El-Badawi, S.A. Ibrahim, M.A. El-Borai, *Arabian J. Chem.* 4 (2011) 37–44.
- [25] S. Sacmaci, S. Kartal, *Anal. Chim. Acta* 623 (2008) 46–52.
- [26] R.A. Singer, M. Dore, J.E. Sieser, M.A. Berliner, *Tetrahedron Lett.* 47 (2006) 3727–3731.
- [27] B.P. Bandgar, S.S. Gawande, R.G. Bodade, N.M. Gawande, C.N. Khobragade, *Bioorg. Med. Chem.* 17 (2009) 8168–8173.
- [28] M. Nagaraju, E.G. Deepthi, C. Ashwini, M.V.P.S. Vishnuvardhan, V.L. Nayak, R. Chandra, S. Ramakrishna, B.B. Gawali, *Bioorg. Med. Chem. Lett.* 22 (2012) 4314–4317.
- [29] R. Craciun, B. Nentwick, K. Hadjiivanov, H. Knozinger, *Appl. Catal. A: Gen.* 243 (2003) 67–79.
- [30] G. Zhang, H. Hattori, K. Tanabe, *Appl. Catal.* 36 (1988) 189–197.
- [31] B.M. Devassy, S.B. Halligudi, S.G. Hegde, A.B. Halgeri, F. Lefebvre, *Chem. Commun.* (2002) 1074–1075.
- [32] O. Meht-Cohn, S. Rhouati, B. Tarnowski, A. Robinson, *J. Chem. Soc. Perkin Trans. 1* (1981) 1537–1543.
- [33] M.S. Park, H.J. Park, K.H. Park, K.I. Lee, *Synth. Commun.* 34 (2004) 1541–1550.
- [34] T. Yamaguchi, *Catal. Today* 20 (1994) 199–218.